CHAPTER 3

Molecular Mechanisms of Cell Death in *Leishmania donovani* Induced by Selected Steroidal Alkaloids

Abstract

Traditionally, individuals afflicted with Visceral leishmaniasis received treatment with miltefosine and amphotericin B, targeting *Leishmania donovani* via apoptosis induction. In the investigation, the efficacy of two steroidal alkaloids, Veratramine and Hupehenine, was assessed in combating the parasite. Contrary to expectations, the study did not detect the typical signs of apoptosis, such as mitochondrial membrane potential loss and phosphatidylserine externalisation. Instead, a notable increase in acidic organelle formation was observed, suggesting a pro-survival response in promastigotes. Through diverse flow cytometric analyses and imaging methods, it was concluded that the parasitic death induced by these natural compounds does not follow the apoptosis pathway but likely involves autophagy. This discovery marks the first instance of autophagy-mediated cell death in *Leishmania donovani* triggered by Veratramine and Hupehenine.

---

*Part of the work published in Journal of Basic Microbiology, 2024. 65(3) e2400655

3.1 Introduction

Leishmania, a unicellular eukaryotic organism belonging to the Trypanosomatidae family, is known for causing numerous infectious tropical diseases, many of which are classified as Neglected Tropical Diseases (NTDs). These diseases, often lethal and lacking effective vaccines, pose significant challenges in terms of treatment. Currently, there are limited therapeutic options available, and instances of relapse and emergence of drug-resistant strains underscore the urgent need for novel treatment strategies. Visceral leishmaniasis (VL), caused by *Leishmania donovani* infection, primarily affects the liver and spleen. Traditional treatments like pentavalent antimonials and meglumine antimoniate have been in use for over 50 years, but their efficacy is limited, particularly in regions like India, where *the Leishmania donovani strain shows* resistance. Alternative treatments such as amphotericin B, paromomycin, and miltefosine have been employed (Kayser et al., 2002; Menpadi et al., 2023; Shalev-Benami et al., 2016; Singh et al., 2014).

In the realm of drug discovery, natural compounds have emerged as promising sources of effective therapeutics. For centuries, natural compounds have been recognised for their rich reservoir of bioactive substances, many of which possess anti-parasitic properties. Examples abound, such as artemisinin, derived from the sweet wormwood plant, which revolutionised malaria treatment in the twentieth century. Similarly, quinine and mefloquine, extracted from the cinchona tree, have been pivotal in combating malaria. Several derivatives of natural products have received FDA approval, including ivermectin for onchocerciasis and niclosamide for tapeworm infection (Cupp et al., 2011; Karbwang et al., 1994; Ofori-Adjei et al., 2008; J. Wang et al., 2019). The previous article described Veratramine and Hupehenine as suitable natural compounds that depicted anti-parasitic activity towards *Leishmania donovani,* targeting dephospho-coenzyme A kinase of the parasite (Menpadi et al., 2023). Veratramine is a lipid-soluble steroidal alkaloid extracted from a flowering herb of the *Veratrum* genus. Many

Veratrum species, like *V. nigrum*, *V. album*, and *V. viride*, etc. have been identified to contain Veratramine. It has been reported that the plant was used in traditional medicine by diverse societies of the world, including China, Greece, Russia and America. It is reported to treat many diseases, from mild illnesses like headache, fever, sore throat, etc., to acute diseases like rheumatism, jaundice, malaria, and so forth (Seale and McDougal, 2022; Shimosaka et al., 2019a; Wen et al., 2015; Zhang et al., 2008). Hupehenine is also a steroidal alkaloid compound extracted from the bulbs of *Fritillaria hupehensis*. Hupehenine has been recorded to be used in traditional Chinese medicine to treat cough and congestion (Menpadi et al., 2023; Seale and McDougal, 2022; Zhang et al., 2008). Hupehenine and its derivatives are reported to show cytotoxicity against cancer cell lines such as HepG2 (human liver cancer cell line), A549 (human lung cancer cell line) and A2780 (human ovarian cancer cell line) (Shimosaka et al., 2019a; Wen et al., 2015).

Veratramine and Hupehenine were sorted by *in-silico* investigations as potential drug compounds against *Leishmania donovani* targeting Dephospho-Coenzyme A Kinase (DPCK). DPCK is the fifth and the last enzyme involved in Coenzyme A biosynthesis that catalyses the conversion of dephospho-Coenzyme A to Coenzyme A (Menpadi et al., 2023). Inhibition of DPCK terminates the production of Coenzyme A, which in turn interrupts the parasite's cellular metabolism and function (Shimosaka et al., 2019b). This includes reduced adenosine triphosphate (ATP) production, impaired cellular energy metabolism, disrupted oxidative phosphorylation, reduced lipid synthesis, impaired protein acylation, interrupted cell proliferation and cell cycle arrest (Leonardi et al., 2005; Robishaw and Neely, 1985). This study aims to provide an overview of Veratramine and Hupehenine as possible drugs against *Leishmania donovani*, emphasising their role in promastigotes' growth and survival.

3.2 Materials and methods

3.2.1 Biological studies

Veratramine and Hupehenine stock suspension were prepared in DMSO (Dimethyl sulfoxide, Sigma). The IC_{50} concentrations of Veratramine and Hupehenine were used as estimated earlier in the published paper. IC_{50} for Veratramine and Hupehenine was 12.5 µM and 7.2 µM, respectively (Menpadi et al., 2023). All the working solutions for biological studies were freshly prepared in M199 media. 1mM H_2O_2 or 100µM H_2O_2 was used as the positive control, and promastigotes without treatment were used as the negative control. All the Flow cytometric experiments were performed with a CytoFlex flow cytometer (Beckman Coulter). 10,000 events per sample were recorded and analysed using CytExpert v 2.4.0.28 software. All of the fluorescence imaging experiments were done with a fluorescence microscope (Olympus BX 63). All the images were analysed using ImageJ 1.54d software.

3.2.2 Cultures and Reagents

Leishmania donovani [MHOM/IN/1983/AG83] was used for the current studies. The promastigotes were grown in M199 media with fetal bovine serum (10%) and antibiotics (100 µg/ml streptomycin and 100 U/ml penicillin) at 25°C in the dark. All the chemicals and reagents used for cell culture were of the highest grade and were acquired from Sigma-Aldrich and Thermofisher Scientific.

3.2.3 Estimation of Reactive Oxygen Species

To estimate the reactive oxygen species (ROS) produced as a result of drug treatment, a cell-permeable fluorescent probe CM-H_2DCFDA (Invitrogen) was used. 2×10^6 (cells/ml) promastigotes were seeded in a 24-well flat-bottom culture plate along with IC_{50} and $2 \times IC_{50}$ drug concentrations (Costa et al., 2020; Mendes et al., 2022c; Saudagar and Dubey, 2014b;

Silva-Silva et al., 2022). The positive and negative controls were also set and incubated for 48 hours at 25°C in the dark. Following incubation, the promastigotes were washed twice with phosphate buffer saline (PBS) and incubated with 5 µM CM-H_2DCFDA for 30min at room temperature (RT). The cells were then washed with PBS, resuspended in 150µl PBS and immediately analysed for their fluorescence intensity using a flow cytometer.

3.2.4 Estimation of Cell Cycle

The effect of drug treatment on the cell cycle was estimated by quantifying the DNA content using nucleic acid staining fluorescent dye propidium iodide (PI, Sigma-Aldrich). *L. donovani* promastigotes (2×10^7 cells /ml) were seeded in a 6-well flat-bottom culture plate preloaded with IC_{50} and $2 \times IC_{50}$ drug compounds, along with the positive and the negative control. The culture plates were incubated for 48 hours at 25°C in the dark. After incubation, the cells were washed twice with cold PBS to remove any residual media, fixed in chilled 70% ethanol (drop-wise), and left overnight at -20°C (Kumar et al., 2017). The fixed promastigotes were centrifuged (5000rpm), washed twice with cold PBS, treated with RNase A (200 µg/ml) and incubated at 37°C for 1h. The cells were then incubated with PI (20 µg/ml) for 20min at RT in the dark. After staining, the cells were immediately analysed using a flow cytometer.

3.2.5 Detection of change in morphology

The effects of drug treatment on the morphology of *L. donovani* promastigotes were determined using a Scanning Electron Microscope (EVO - Scanning Electron Microscope MA15/18, ZEISS). 2×10^6 (cells/ml) promastigotes were seeded in a 24-well flat-bottom culture plate preloaded with drugs along with the positive and the negative controls. After 48 hours of incubation, cells were washed twice with phosphate buffer (PB) and fixed in 2.5% glutaraldehyde (GA), overnight at 4°C (Fischer et al., 2012). The cells were later washed with

PB and subsequently with ultrapure water. After serial dehydration, the cells were analysed under a Scanning Electron Microscope (SEM).

3.2.6 Detection of phosphatidylserine externalisation

The translocation of phosphatidylserine (PS) from the inner to the outer surface of the plasma membrane is a characteristic feature of early apoptosis. This is detected by Annexin-PI dual-staining, which is used to evaluate the apoptosis-inducing capacity of the drugs. Promastigotes were stained with Annexin V and PI according to the manufacturer's instructions (FITC Annexin V/ Dead cell Apoptosis kit, Invitrogen). Briefly, 2×10^6 (cells/ml) treated and untreated cells were centrifuged, washed twice with cold PBS and resuspended in 100µl 1 X annexin-binding buffer. Later, the promastigotes were stained with FITC Annexin V and PI and incubated at RT for 15 min. After incubation, 400µl 1 X annexin-binding buffer was added, gently mixed and immediately analysed in the flow cytometer.

3.2.7 Estimation of Mitochondrial-membrane potential

The mitochondrial membrane potential (MMP) was estimated using MitoTracker Red CMXRos (Invitrogen), a cell-permeable fluorescent dye that labels mitochondria in live cells. After 48h, treated and untreated promastigotes (2×10^6 cells/ml) were washed with M199 incomplete media and incubated with MitoTracker Red CMXRos (200nM) for 10min under growth conditions in the dark. The cells were washed with PBS, fixed in PFA (4%) and analysed under the fluorescence microscope.

3.2.8 Estimation of acidic organelles

Acridine orange (AO) is an organic compound which selectively binds to nucleic acids and emits green fluorescence. At lower pH, AO penetrates acidic organelles and emits red fluorescence. The acidic organelles generated in the cells lead to a cascade of products for

phagocytosis of damaged components (Thomé et al., 2016). Treated promastigotes (2×10^6 cells/ml) and controls were incubated for 48 hours and washed twice with PBS. Next, the promastigotes were stained with AO (5µg/ml, Sigma-Aldrich) for 15min at RT in the dark. The cells were washed twice with PBS and fixed with 4% paraformaldehyde (PFA) for 10min at RT. The fixed cells were analysed under the fluorescence microscope.

3.2.9 Determination of gene expression

The change in gene expression was estimated by quantitative real-time polymerase chain reaction (RT-qPCR). The total RNA from 1×10^7 cells/ml after 48 hours of treatment was extracted by the manual method using TRIzol (Invitrogen). The promastigotes were washed twice with chilled PBS and lysed using cold TRIzol. Phase separation was done using the chloroform method, and the upper aqueous phase containing RNA was precipitated with isopropanol. Finally, the RNA pellet was washed with 75% ethanol and eluted. The total RNA was quantified using nanodrop, and cDNA synthesis was carried out using 1µg of RNA from each treatment using RevertAid First Strand cDNA Synthesis Kit (Thermoscientific) according to the manual.

The quantitative gene expression analysis was estimated by RT-qPCR using PowerUp SYBR Green Master Mix (Applied Biosystems, Life Technologies). Gene-specific forward and reverse primers were used along with an equal volume of cDNA for RT-qPCR. Real-time monitoring was detected using a 7500 real-time PCR system (Applied Biosystems). Alpha tubulin was used as an internal control for real-time monitoring of gene expression.

3.2.10 Detection of autophagic vacuoles

The induction of autophagy is marked by the formation of double-membrane vesicles, autophagosomes, which fuse to lysosomes to form autophagolysosomes. These vesicles or autophagic vacuoles were detected by staining with a CYTO-ID Autophagy detection kit (Enzo

Life Sciences) according to the manufacturer's instructions. In brief, 2×10^6 cells/ml treated and untreated promastigotes, for 48h, were washed twice with 1X assay buffer and incubated with dye (Hoechst 33342 and CYTO-ID) for 30min at 37˚C. The promastigotes were fixed in 4% PFA after washing with 1X assay buffer. The fixed parasites were visualised under a fluorescence microscope.

3.2.11 Statistical analysis

The samples were analysed with at least two independent experiments. The flow cytometric values were expressed as a percentage of cells for each marker compared to the total number of cells ± standard error of the mean (SE) using OriginPro 2023b software. The data was analysed using a two-way ANOVA test with different significance levels (**: $p < 0.05$, *: $p < 0.1$). ImageJ 1.54d software was used to analyse the fluorescence images.

3.3 Results

3.3.1 Analysis of Reactive Oxygen Species

To evaluate the change in ROS production in cells as a result of drug treatment, CM-H_2DCFDA dye was used. ROS is produced as a consequence of oxidative stress generated in the cells. After 48 hours of treatment with drugs, promastigotes have shown increased ROS production as compared to the untreated control. An increase in ROS levels at $2 \times IC_{50}$ concentrations of both drugs was observed, with a higher percentage estimated in Veratramine (33.23 ± 2.95 %) than in Hupehenine (19.60 ± 0.86 %) (Figure 15).

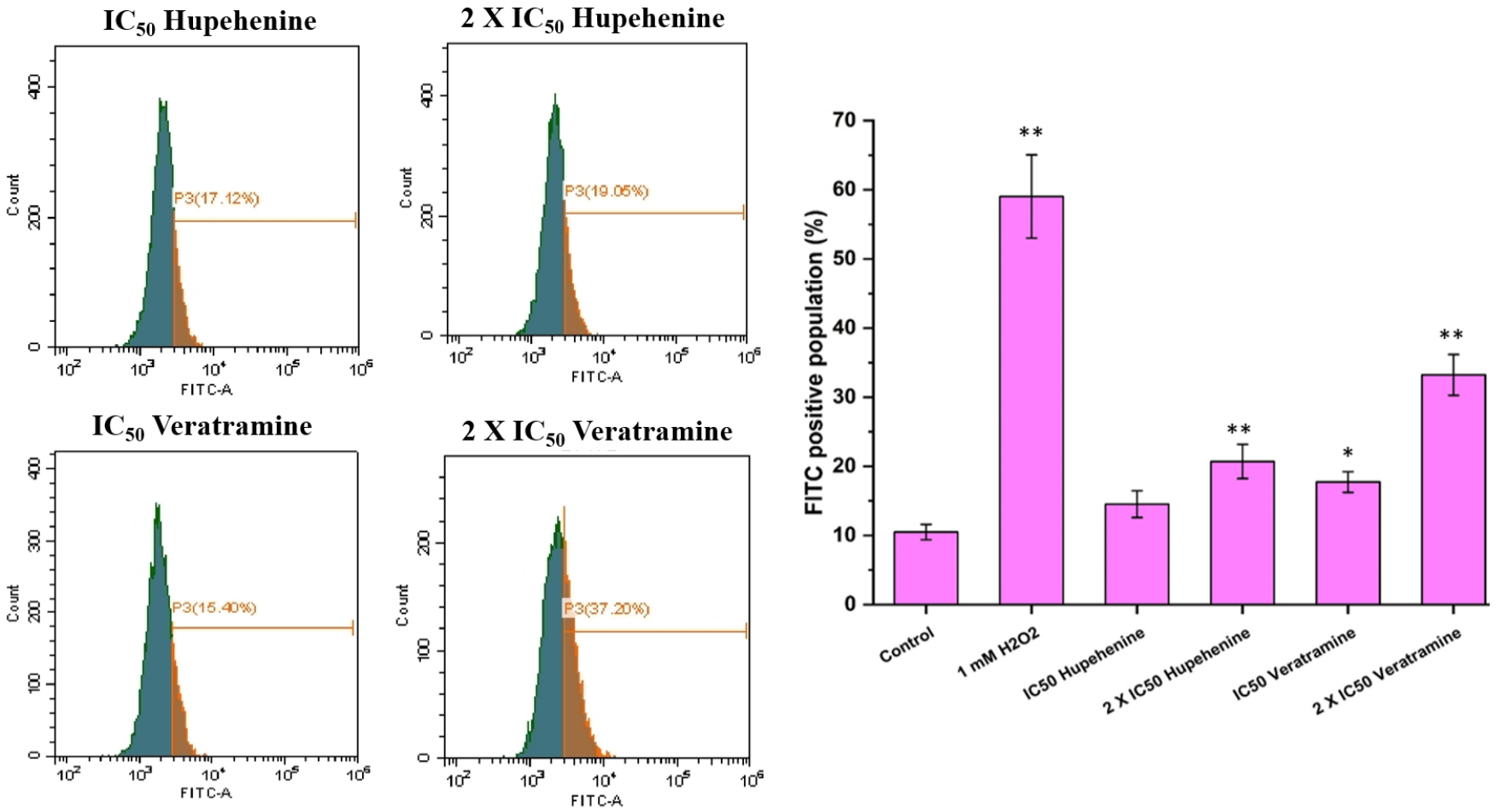

Figure 15: Evaluation of ROS levels produced after 48 hours of treatment with IC_{50} and 2× IC_{50} concentrations of hupehenine and veratramine. H_2O_2 (1mM) is considered a positive control, and untreated promastigotes were considered a negative control. Significant differences were considered concerning the untreated parasite (control), where $p \leq 0.10$ (*) and $p \leq 0.05$ (**).

3.3.2 Cell-cycle analysis

The effect of drug treatment on the cell cycle was evaluated by PI staining, which displays the DNA content of the cell population. Compared to the untreated cells, up to 30% and 50% increases in the G1 phase of the cells were calculated with 2 × IC_{50} concentrations of Hupehenine and Veratramine, respectively. It was noticed that there is an increase in the G1 phase of the treated promastigotes, which accelerates with an increase in drug concentration (Figure 16). This suggests that there is DNA damage in the presence of Hupehenine and Veratramine, and the cells are arrested at the G1 phase of the cell cycle.

3.3.3 Cellular morphology analysis

The change in morphology of *L. donovani* promastigotes in the presence of drugs was observed under SEM, and the ultrastructures of the parasites were captured. A drastic change in the morphology of *L. donovani* promastigotes was observed with an increase in drug concentration. After 48 hours of treatment with the drugs, swelling and distortion of cells were witnessed. Flagellar abnormalities and loss were also spotted, especially in the presence of Veratramine than in Hupehenine (Figure 17).

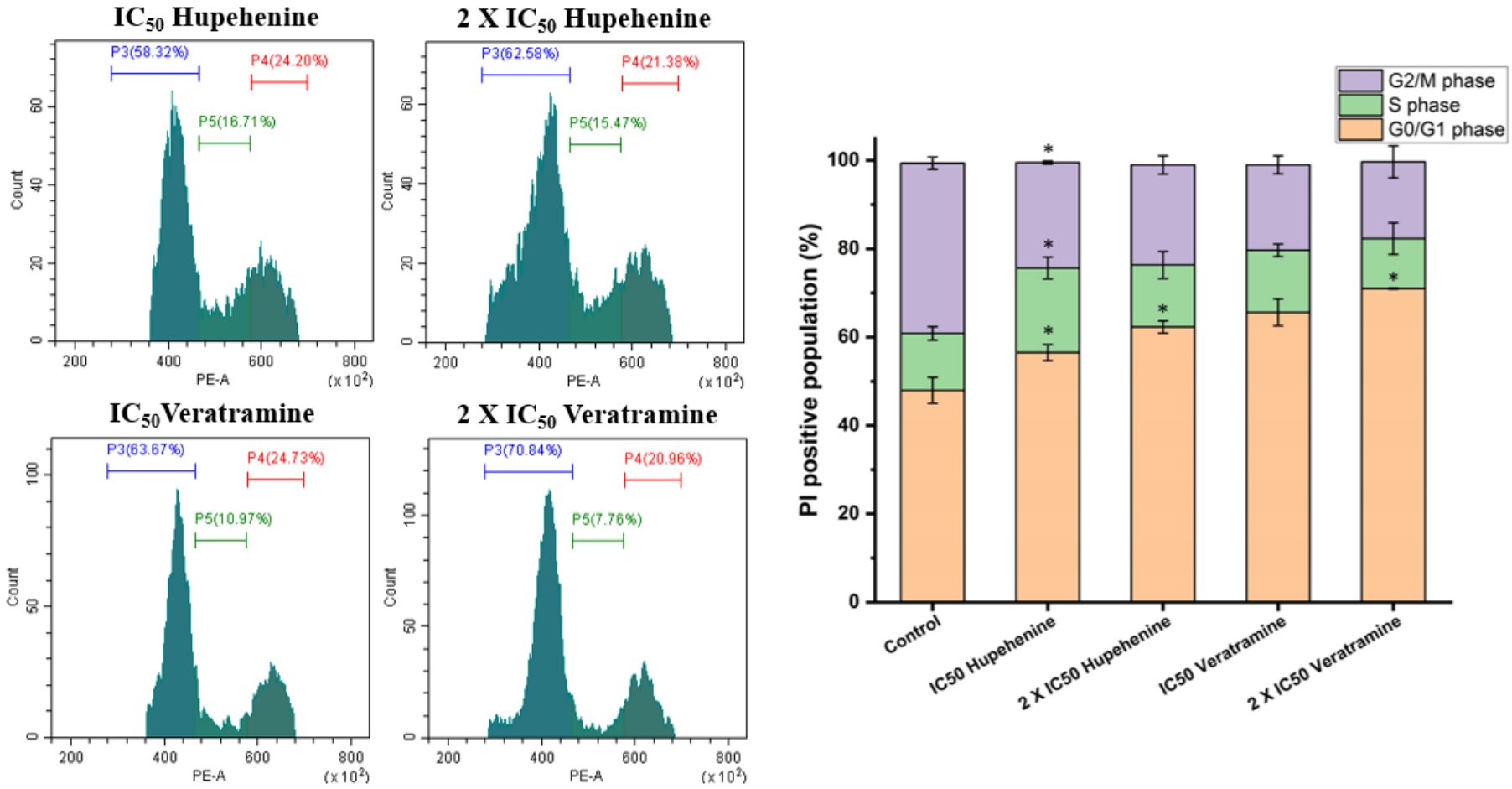

Figure 16: Cell cycle analysis of *L. donovani* by DNA staining using PI after 48 hours of treatment with IC_{50} and 2× IC_{50} concentrations of hupehenine and veratramine. Untreated promastigotes were taken as a positive control. Significant differences were considered concerning the untreated parasite (control), where $p \leq 0.10$ (*) and $p \leq 0.05$ (**).

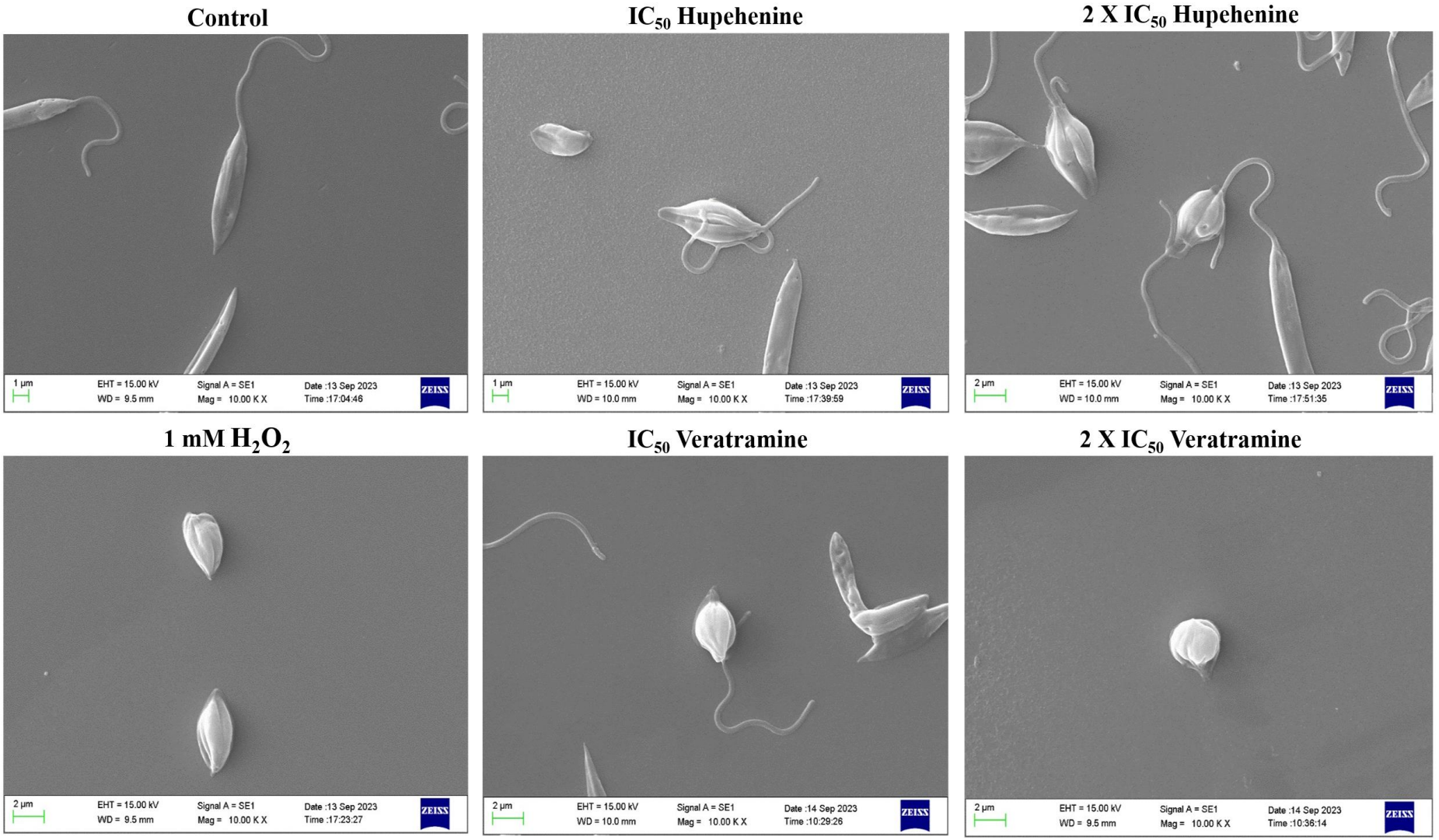

Figure 17: Ultrastructural changes identified in promastigotes through Scanning Electron Microscope. Alteration in cell morphology was observed after treatment with Hupehenine and Veratramine.

3.3.4 Examination of phosphatidylserine externalisation

Flipping of PS from the cytoplasmic membrane's inner surface to the membrane's outer surface is a classic indication of early apoptosis in higher eukaryotes. Annexin V phospholipid-binding protein has a high affinity towards PS and, therefore, is used to detect PS externalisation. Counterstaining with PI is done to stain exposed DNA to distinguish necrotic cells from apoptotic cells. There was an increase in the percentage of apoptotic cells at 2 × IC_{50} concentrations of both drugs (31.24 ± 0.34 for Hupehenine and 28.67 ± 2.52 for Veratramine) than at their IC_{50} concentrations (Figure 18). There were more apoptotic cells (early + late) when treated with Hupehenine compared to Veratramine.

3.3.5 Analysis of Mitochondrial-membrane potential

MMP plays an essential role in the smooth functioning of the mitochondria and other metabolic regulations of the cell. The change in MMP was detected by MitoTracker Red CMXRos, which labels healthy mitochondria, giving red fluorescence. The fluorescence emitted by the *L. donovani* promastigotes was examined by a fluorescence microscope. Considering fluorescence intensity in untreated control as 100%, the loss in MMP was estimated to be around 55% and 10% at IC_{50} concentrations of Hupehenine-treated promastigotes and Veratramine-treated promastigotes, respectively. However, it was observed that there is less loss of MMP at 2 × IC_{50} concentrations of Hupehenine (around 25%) and almost no change in MMP at 2 × IC_{50} concentrations of Veratramine (Figure 19).

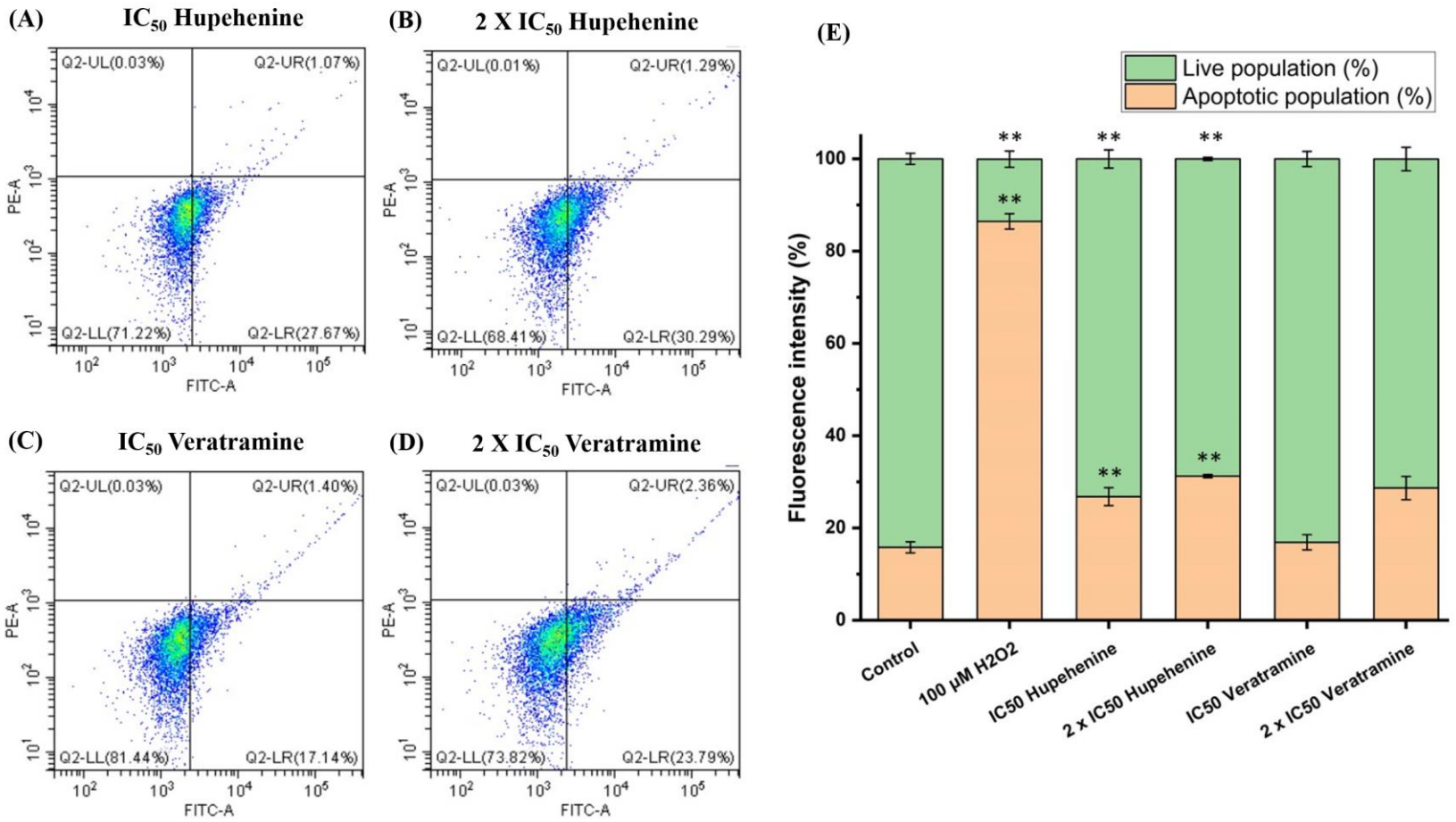

Figure 18: Externalisation of phosphatidylserine analysed by Annexin V -PI staining after 48 hours of treatment. (A) IC_{50} concentration of Hupehenine, (B) 2 × IC_{50} of Hupehenine, (C) IC_{50} concentration of Veratramine, (D) 2 × IC_{50} of Veratramine, and (E) Stacked graphical representation of total apoptotic (early apoptotic and late apoptotic cells) and live promastigotes after treatment. 100µM H_2O_2 was used as a positive control.

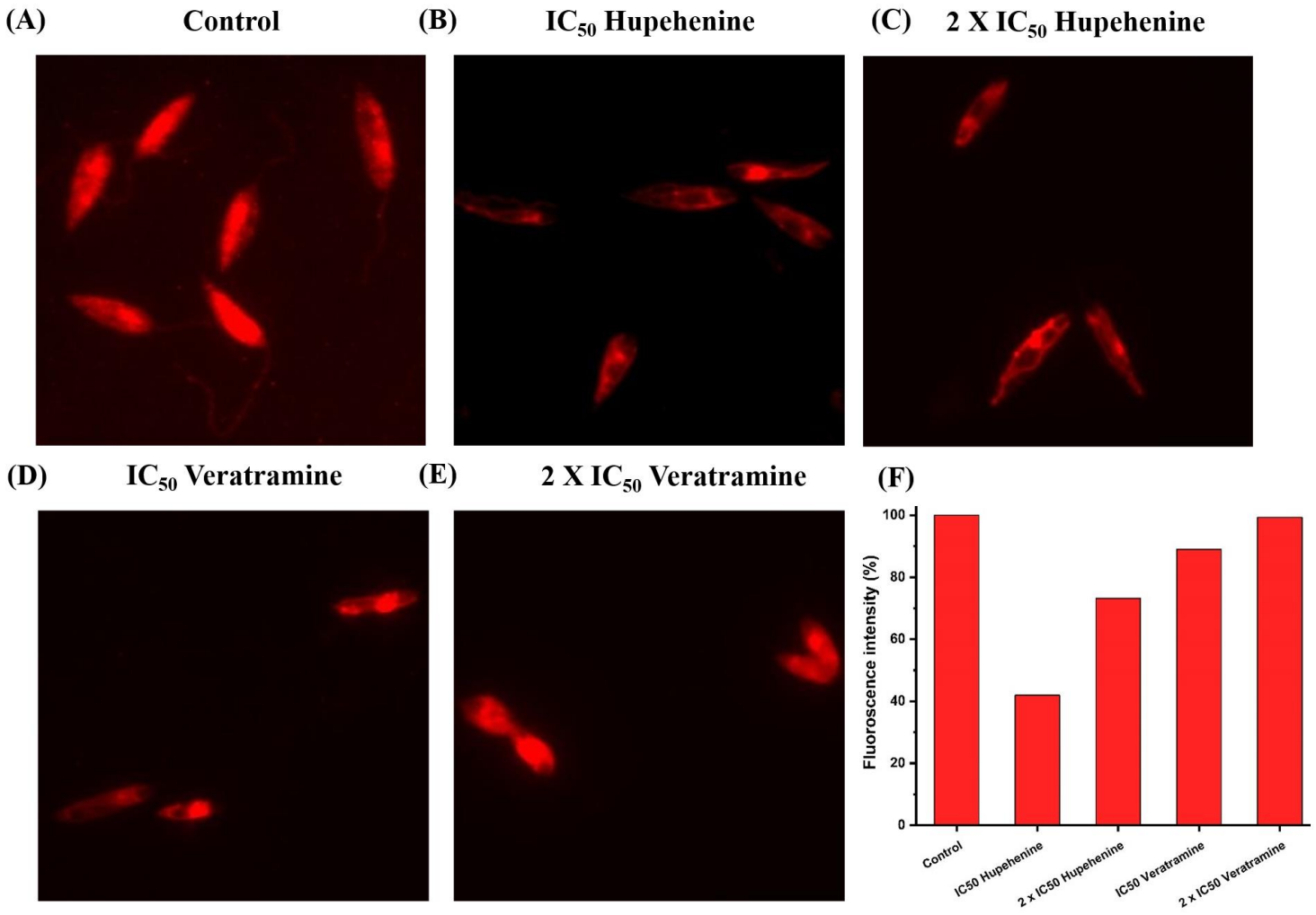

Figure 19: Assessment of mitochondrial membrane potential by a fluorescent probe through a fluorescence microscope. (A) Untreated control, (B) IC_{50} concentration of Hupehenine, (C) 2 × IC_{50} concentration of Hupehenine, (D) IC_{50} concentration of Veratramine, and (E) 2 × IC_{50} concentration of Veratramine, and (F) Graphical representation of mitochondrial membrane potential indicated by Mitotracker Red CMXRos. The fluorescence intensity produced by the control was considered to be 100%.

3.3.6 Analysis of acidic organelles

AO is a cell-permeable fluorescent dye with cationic properties that labels DNA and emits green fluorescence. However, AO is also stable in acidic pH and has the potential to enter membrane-bound acidic organelles such as lysosomes and phagolysosomes. These organelles are functional during acid hydrolysis and synthesising compounds involved in the phagocytosis of damaged components. This versatile nature of AO has been used to distinguish between viable and damaged cells. AO stains viable cells green as it binds to the nucleus and damaged cells red because of the acidic organelles. This red fluorescence diminishes in necrotic cells due to ruptured and leaky lysosomes. The fluorescence emitted by the AO-stained promastigotes was examined by a fluorescence microscope. It was observed that there is an increase in the intensity of red fluorescence in the presence of drugs, and it intensifies at higher concentrations (Figure 20 (A)). Considering the red fluorescence detected by promastigotes treated with 100µM H_2O_2 as the maximum intensity, the promastigotes treated with IC_{50} Hupehenine, 2 × IC_{50} Hupehenine, IC_{50} Veratramine and 2 × IC_{50} Veratramine exhibited 45.5%, 85.2%, 36% and 78.5 % red fluorescence, respectively (Figure 20 (B)). This implies that Hupehenine induces more acidic organelle production than Veratramine.

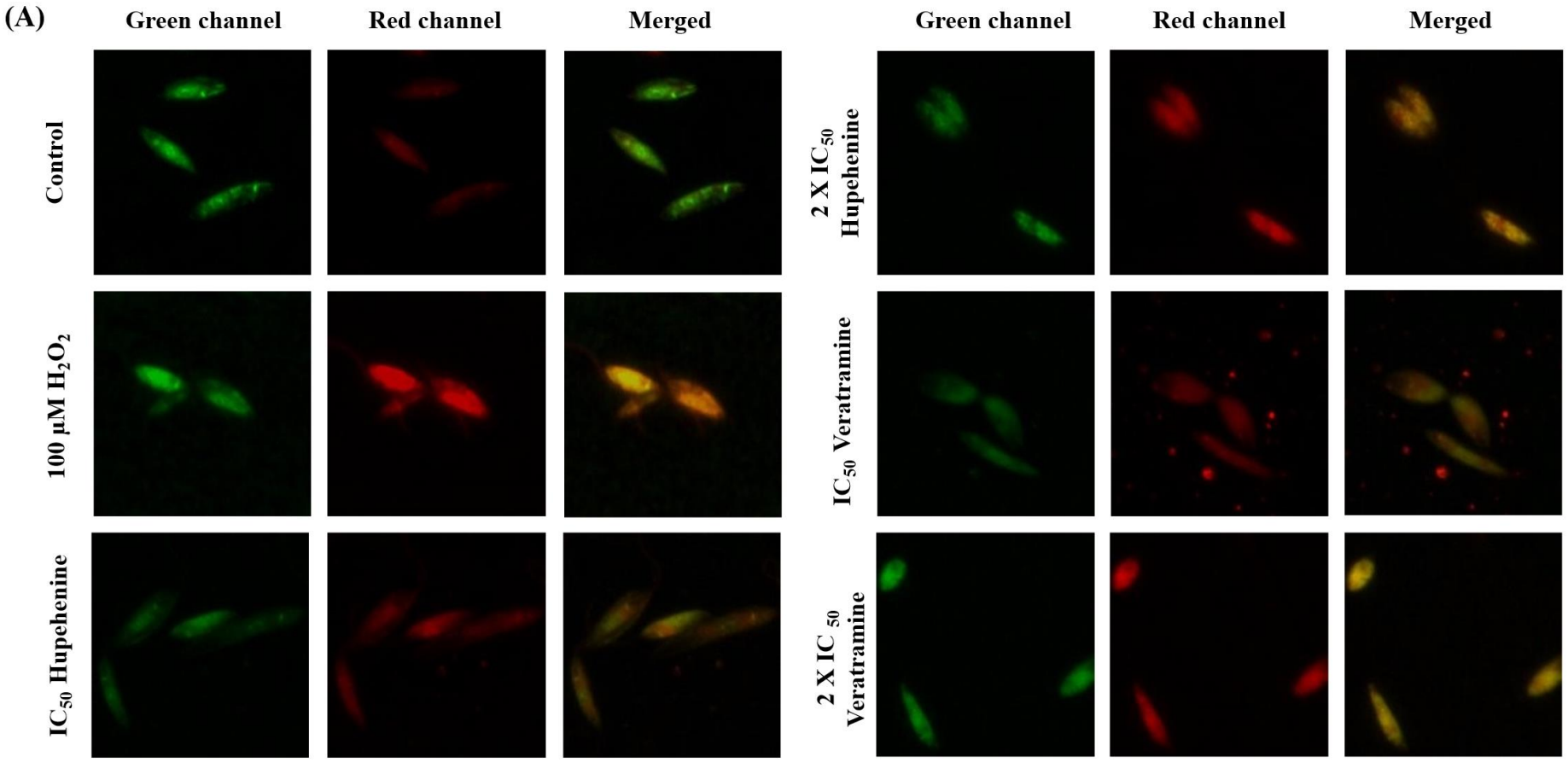

Figure 20 (A): Acridine orange staining indicates acidic organelle production through drug treatment. Image panel representing the increase in acidic vacuole production after drug treatment at IC_{50} and 2 × IC_{50} concentrations. Untreated parasites were used as a negative control, and H_2O_2 was used as a positive control. (Background noise in fluorescence images has been cancelled for illustration purposes only)

(B)

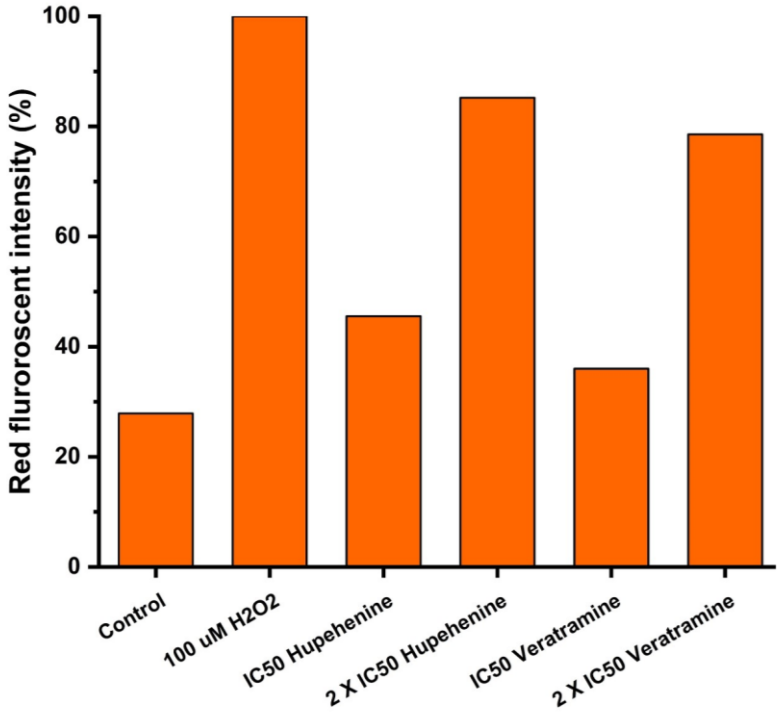

Figure 20 (B): Acridine orange staining indicates acidic organelle production through drug treatment. Graphical representation of acidic organelle observed through the red channel. Untreated parasites were used as a negative control, and H_2O_2 was used as a positive control. H_2O_2 was considered to have a 100% red fluorescence intensity to ease the interpretation.

3.3.7 Estimation of change in gene expression

The evidence for autophagy induced by the drugs was observed at the mRNA level using the RT-qPCR technique. The genes involved in autophagic vacuole formation were used as markers for autophagy induced by Hupehenine and Veratramine. Autophagic vacuole formation is regulated by a set of ATG proteins, including ATG4, ATG5, ATG7, ATG8 and ATG12. In *Leishmania sp*., the families of ATG8 genes are reported: ATG8A, ATG8B, ATG8C and ATG8 (Giri and Shaha, 2019; Singh et al., 2017). The expression of ATG7, ATG8A and ATG8B genes was quantified to explain the autophagic vacuole formation due to drug treatment. Alpha-tubulin was used as an internal control. After 48 hours of treatment with Hupehenine and Veratramine, it was observed that there was an increase in the expression of ATG7 and ATG8B genes, which indicates that autophagic vacuoles are induced (Figure 21). However, the ATG8A gene expression was low, which could be explained by post-transcriptional modifications and protein stability in promastigotes (Cortazzo da Silva et al., 2022; Karamysheva et al., 2020).

3.3.8 Detection of autophagic vacuoles

The autophagic vacuole formation as a result of drug treatment was tracked using CYTO-ID dye, a cationic amphiphilic probe, which specifically stains autophagic vacuoles and excites at 488nm. Microscopic observations showed increased CYTO-ID-stained promastigotes after 48 hours of treatment with IC_{50} and 2 × IC_{50} concentrations of Hupehenine and Veratramine (Figure 22 (A)). There is more than 10% and 30% increase in autophagic vacuole induction in promastigotes treated with IC_{50} concentrations of Hupehenine and Veratramine, respectively, as compared to untreated control, and the value increases at higher concentrations (Figure 22 (B)).

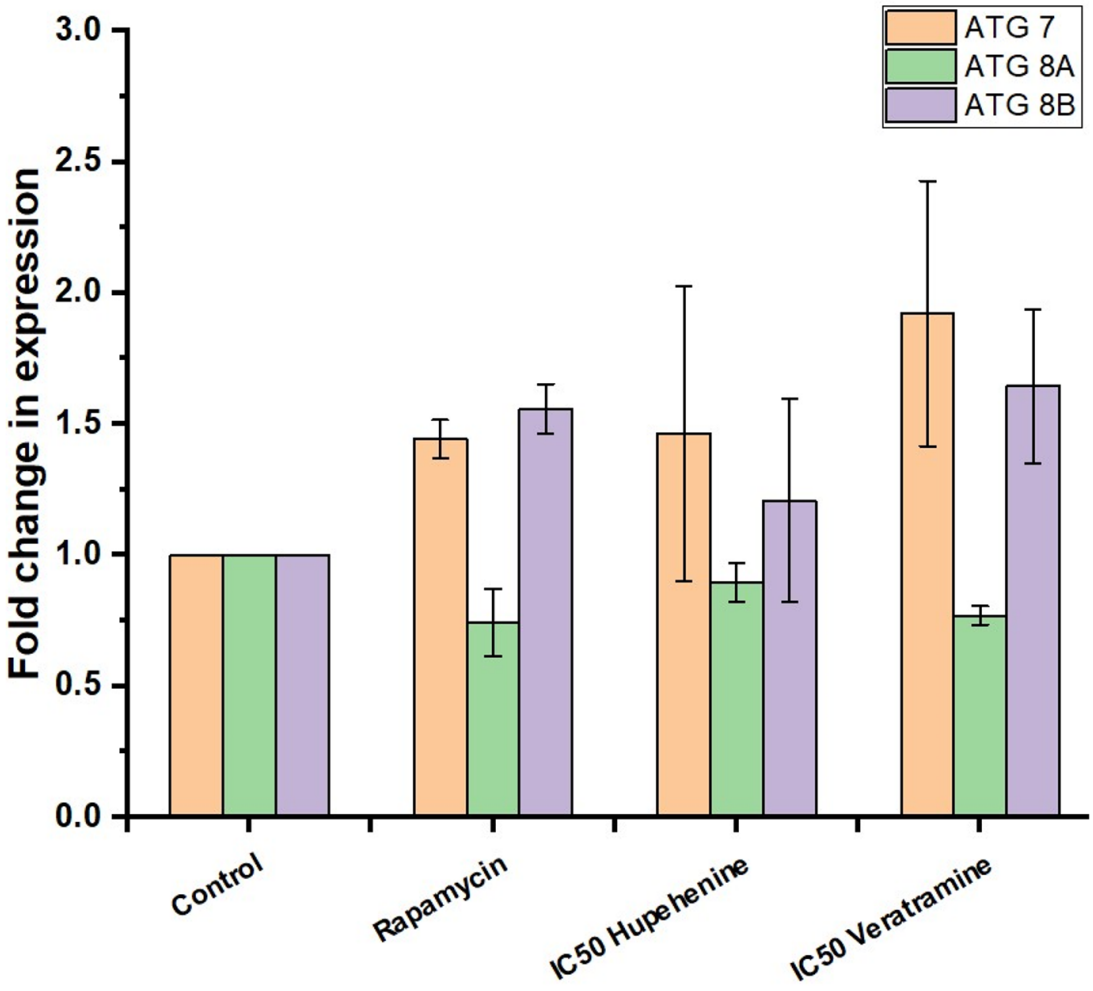

Figure 21: Quantitative profiling of gene expression of major autophagic genes (ATG7, ATG8A and ATG8B) by RT-qPCR after 48 hours of treatment with IC_{50} concentration of Hupehenine and Veratramine. Rapamycin was considered a positive control, and untreated parasites were considered a negative control.

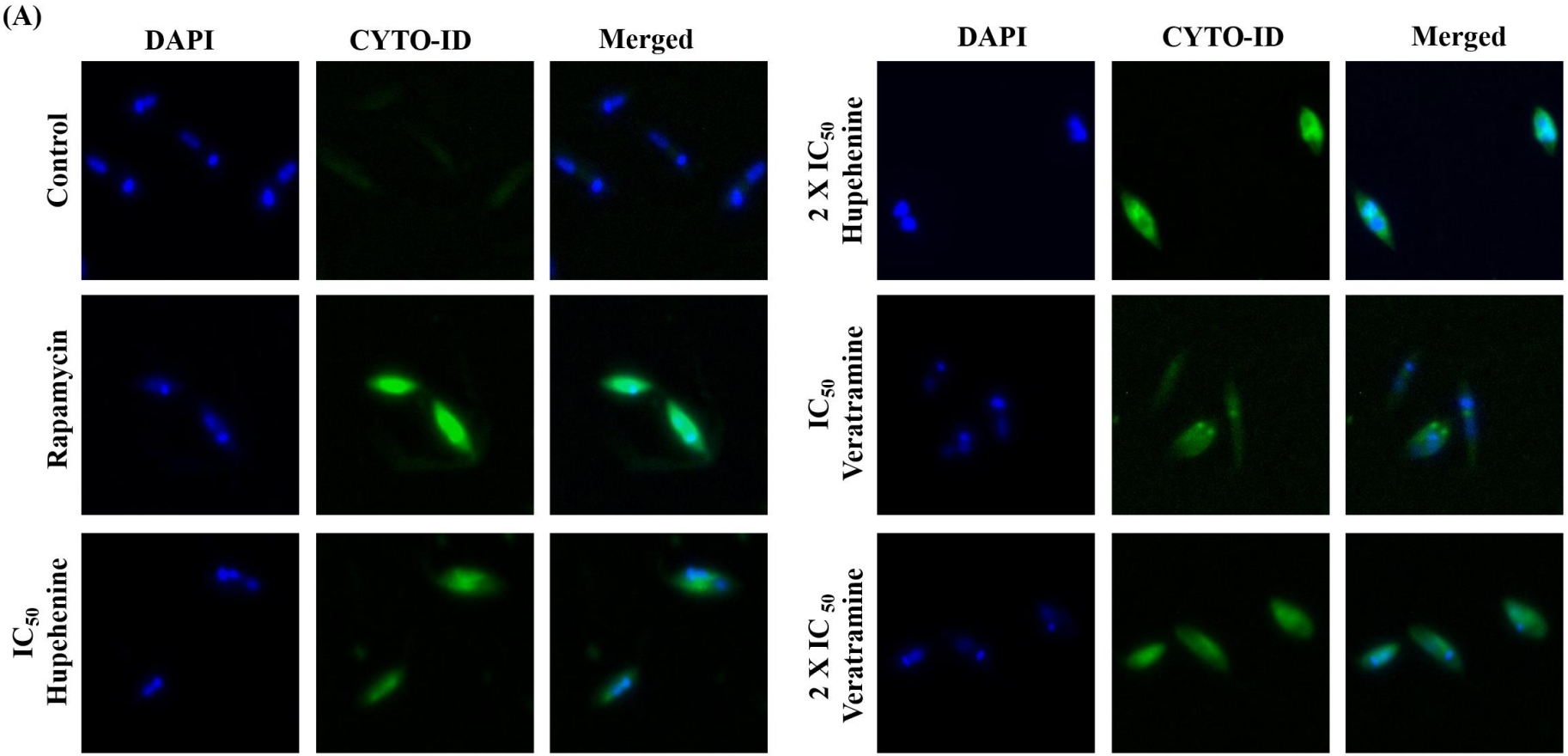

Figure 22 (A): Evaluation of accumulated autophagic vacuoles through fluorescence imaging. Promastigotes treated with IC_{50} and 2 × IC_{50} concentration of Hupehenine and Veratramine were stained with CYTO-ID dye for the autophagic vacuoles and Hoechst 33342 for the nucleus. Promastigotes treated with Rapamycin were used as a positive control, and untreated promastigotes were used as a negative control. (Background noise of the fluorescence images has been cancelled, and contrast has been improved for illustration purposes only)

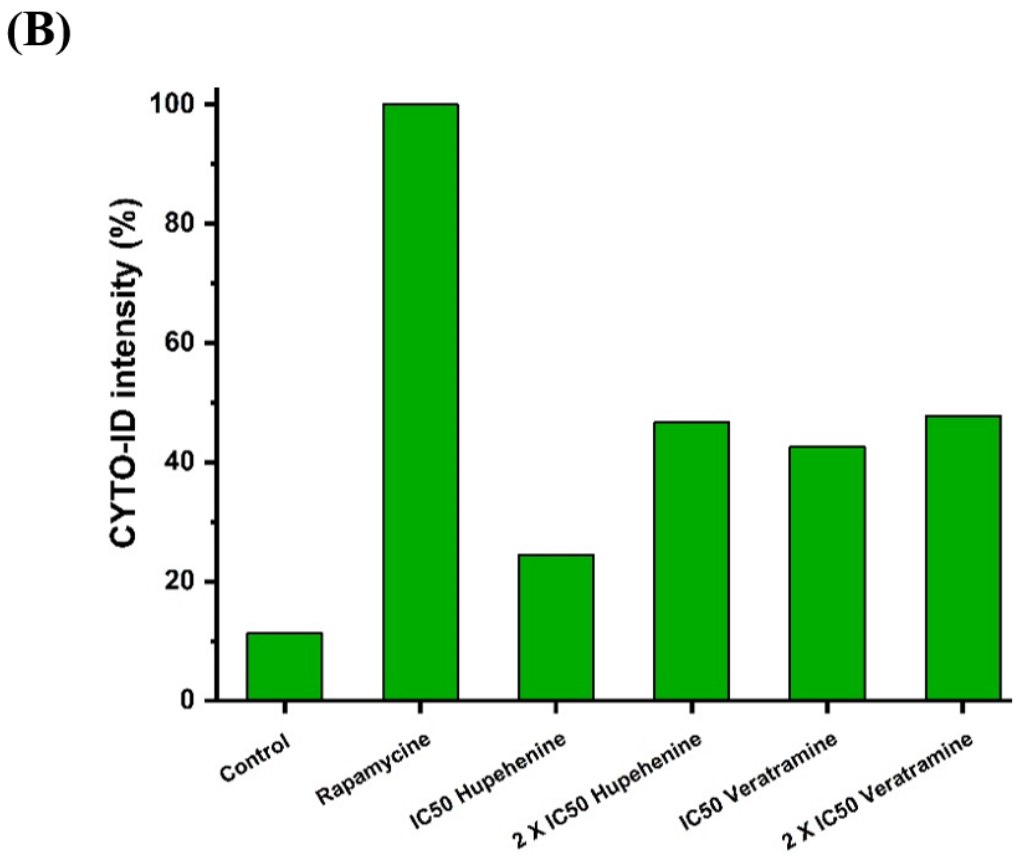

Figure 22 (B): Evaluation of accumulated autophagic vacuoles through fluorescence imaging. Graphical representation indicating the relative fluorescence intensity of CYTO-ID stained parasites after 48 hours of treatment. The fluorescence intensity of the Rapamycin-treated parasite is considered 100% for comparison

3.4 Discussion

Patients afflicted with VL typically receive treatment involving the administration of a polyene antibiotic, amphotericin B, and an alkyl-phospholipid, miltefosine (Kayser et al., 2002). Both amphotericin B and miltefosine have been documented to induce apoptosis-like cell death in *Leishmania donovani* (Mendes et al., 2022; Paris et al., 2004). Apoptosis, a genetically regulated form of programmed cell death initially believed to be exclusive to multicellular eukaryotes, has been identified in unicellular eukaryotes, including various species of *Leishmania*, such as *Leishmania donovani* (Bera et al., 2003; Lyu et al., 2015). Classical indicators of apoptosis in *Leishmania* encompass cell shrinkage, nuclear condensation, DNA fragmentation, loss of mitochondrial membrane potential, release of mitochondrial cytochrome c, increased reactive oxygen species, and release of caspase-like proteases (Basmaciyan & Casanova, 2019; Neto et al., 2011; Paris et al., 2004). Autophagy, a conserved mechanism in eukaryotes crucial for maintaining cellular homeostasis and coping with cellular stress, involves the degradation of cellular contents such as organelles, proteins, and macromolecules in lysosomes, followed by recycling for biomolecule synthesis (Bera et al., 2003; Lyu et al., 2015). The interplay between autophagy and cell survival is intricate and contingent upon various factors. While autophagy can serve as a pro-survival mechanism under certain circumstances by eliminating damaged cellular components and promoting cell viability, excessive or prolonged autophagy in stressful conditions may lead to cell death, known as autophagy-mediated cell death or type II programmed cell death (Lyu et al., 2015).

In the investigation, treatment with IC_{50} Hupehenine and IC_{50} Veratramine led to a ROS increase of no more than 20%. The cell cycle arrest was detected at the G1 phase in *L. donovani* promastigotes following exposure to Veratramine and Hupehenine, evidenced by an elevated G1 population. This suggests that these drugs impede growth and proliferation, which is further

supported by morphological alterations like cell swelling, distortion, flagellar abnormalities, and flagellar loss observed through SEM. To explore whether cell death is mediated by apoptosis, phosphatidylserine externalisation and mitochondrial membrane potential (MMP) were examined. While the number of FITC-positive cells increased with rising drug concentrations, they did not exceed 30%. The change in MMP also did not conform to the classical apoptosis pattern. Specifically, higher drug concentrations did not consistently lead to decreased MMP and subsequent cellular respiration decline, a hallmark of apoptosis. Interestingly, at higher drug concentrations ($2 \times IC_{50}$), there was no significant MMP loss, contrary to lower concentrations (IC_{50}). This suggests that molecular mechanisms promoting increased autophagy may counteract cellular distress collectively, potentially allowing *L. donovani* mitochondria to restore MMP at higher drug concentrations (Haeussler et al., 2020).

Gene expression levels do not always align with protein expression levels due to regulatory processes post-to-mRNA synthesis, involving post-transcriptional and post-translational modifications. For instance, a low translation rate can yield highly stable proteins, resulting in high cellular concentrations, and vice versa. This discrepancy could explain the findings regarding the ATG8A gene (Greenbaum et al., 2003; Karamysheva et al., 2020). However, increased expression of ATG7 and ATG8B genes corresponds with enhanced autophagic vacuole staining using CYTO-ID dye after treatment with IC_{50} concentrations of both Hupehenine and Veratramine (Giri & Shaha, 2019; Liu et al., 2023; Singh et al., 2017). Thus, while the drugs induce cell death in *L. donovani*, it appears to be a form of programmed cell death distinct from apoptosis (type I programmed cell death). The MMP data pattern suggests a cellular attempt to withstand increased or extreme stress, potentially indicating autophagy, a pro-survival mechanism. Prolonged stress-induced autophagy is characterised by extensive cytoplasmic vacuolization, eventually leading to self-destruction and cell death. This is further supported by increased acidic organelle and autophagic vacuole formation in *L. donovani*

promastigotes at 2 × IC_{50} drug concentrations compared to IC_{50} drug concentrations (Neto et al., 2011; Thomé et al., 2016). Cell cycle arrest, morphological abnormalities, and autophagic organelle production validate the direct association of cell death with autophagy.

Evidence has shown Veratramine toxicity in human GBM cell lines, primarily through G0/G1 phase cell cycle arrest and inhibition of the PI3K/Akt/mTOR signalling pathway (Kim et al., 2022; Seale & McDougal, 2022). Additionally, it has been found to hinder prostate cancer proliferation via the ATM/ATR and Akt pathways. Veratramine also exhibits hypotensive and analgesic effects, surpassing the efficacy of common analgesic drugs like pethidine (Li et al., 2019; L. Wang et al., 2008). Yin *et al.* revealed Veratramine's ability to impede liver cancer proliferation through autophagy-mediated apoptosis by suppressing the PI3K/Akt/mTOR signalling pathway (Yin et al., 2020b). Traditionally, Hupehenine is used in Chinese medicine to alleviate colds and congestion. It also shows promising therapeutic effects against neurodegenerative diseases (Ghanem et al., 2021). Pharmacokinetic studies report a bioavailability of 13.4% for Hupehenine (Wen et al., 2015). In addition to the steroidal alkaloids discussed here, antimicrobial peptides have been identified as agents capable of activating autophagy-mediated cell death in *Leishmania donovani* (Bera et al., 2003).

In summary, Veratramine and Hupehenine effectively hinder the growth and proliferation of *L. donovani* promastigotes. The flow-cytometric and microscopic examinations suggest that this inhibitory effect does not stem from apoptosis-like cell death; rather, the analysis indicates it arises from autophagy-mediated cell death. Further validation of the role of these steroidal alkaloids in autophagy-mediated cell death in *Leishmania donovani* is warranted, necessitating time-dependent proteomic studies employing multiple markers to corroborate the current findings. Nevertheless, Veratramine and Hupehenine hold promise for exploration against other closely related parasitic diseases such as sleeping sickness and chagas disease.